COMPDYN 2011
III ECCOMAS Thematic Conference on
Computational Methods in Structural Dynamics and Earthquake Engineering
M. Papadrakakis, M. Fragiadakis, V. Plevris (eds.)
Corfu, Greece, 25–28 May 2011

DIMENSIONAL STABILITY LOSS IN STRUCTURES SUBJECT TO RANDOM VIBRATION

Ruben L. Edeson[1], Guglielmo S. Aglietti[2], Adrian R. Tatnall[2]

[1] RAL Space
STFC Rutherford Appleton Laboratory, Harwell Oxford, Didcot, OX11 0QX, UK
e-mail: ruben.edeson@stfc.ac.uk

[2] School of Engineering Science, University of Southampton
Highfield, Southampton, SO17 1BJ
email: gsa@soton.ac.uk; art4@soton.ac.uk

Keywords: Dimensional Stability, Random Vibration, Cyclic Plasticity.

Abstract. *Highly stable structures that are destined for space use are vulnerable to dimensional stability loss due to random vibration loads experienced during launch and ground testing. Small movements at structural interfaces and non-recoverable strains induced in metering elements can have negative implications for optical performance on-orbit.*

Often the dimensional stability aspects of optical bench structures are verified by environmental tests on Engineering or Protoflight Model instruments. It is proposed that a better understanding of vibration-induced structural dimensional stability loss could enable the assessment of stability loss through analysis at an early stage.

To this end, several tests have been developed at RAL to assess dimensional stability loss in materials and joints in a controlled manner under random vibration. One test has been used to assess Al alloy and CFRP material samples in a 4-point bending configuration, and another has been used to assess micron-level slipping at a bolted interface.

The aim of these tests was to provide useful material data, and also to assess the feasibility of predicting stability loss caused by random vibration events. It was found that the classical frequency domain random vibration Finite Element Analysis commonly performed to assess safety margins against structural failure on space structures is probably insufficient to predict instability. This is because the results are highly dependent on non-symmetry in the stress response (ie, due to gravity, pre-stress, or non-linear response). However a good correlation with test results was achieved with a time domain FEA model which incorporates nonlinear kinematic hardening rules in the materials.

This paper will outline the Al alloy sample test and results, as well as propose a way to estimate random vibration-induced dimensional stability loss using static microyield test results.

1 INTRODUCTION

Optical instruments used in space typically require that vital components are maintained in alignment within certain tolerances throughout their operational lifetime in order to guarantee adequate system performance. This is particularly true for low-cost Earth observation missions which seek to package large optics in small lightweight instruments with minimal or no need for on-orbit readjustment mechanisms.

For a camera structure which is aligned in a ground based cleanroom, a number of potential sources of instability exist during the ground test, launch and operational phases. Thermal expansion is possibly the most significant, driving the use of low expansivity materials such as CFRP. Moisture desorption is another issue, as are gravity release, creep, erosion by atomic oxygen, and dynamic loads during launch. This paper deals with the last of these effects.

Payload structures are subject to a period of dynamic loading during launch. These loads originate from aeroacoustic noise and stage separation events. During the design and development of such structures, there is often some uncertainty over the exact vibration levels that will be witnessed during launch. This leads to potentially high qualification test specifications. These test specifications can be used to dimension a structure in the early part of the design process, and validate it against gross structural failure using Finite Element Analysis (FEA). Dimensional stability failures due to random vibration can be harder to assess however, and this aspect of the design is usually verified by test at a later stage.

This paper seeks to introduce methods of reducing the risk to structural dimensional stability earlier in the development process, using FEA methods. It draws on the test results of some dimensional stability tests recently performed at RAL, and demonstrates that these can be replicated with a simple FEA model using cyclic plasticity material properties.

2 TEST DESCRIPTION

The aim of the test was to investigate the dimensional stability response of various material samples to random vibration. The material described here is aluminium alloy 2024 T3.

The test setup made use of a simply supported material test sample in strip form. There were a pair of masses attached inboard of the support positions (see Figure 1). The sample was then subject to random vibration in the direction that induces bending in the strip. The masses were selected such that the first modeshape of the sample approximates a standard four-point bending test, at a frequency of 41 Hz. Three identical samples were tested simultaneously, using an LDS V8-440 SPA56K shaker.

The simple support was achieved by clamping the samples between a pair of stainless steel rods at each support point (see Figure 2). The clamping force was achieved using extension springs. The spring force was determined to be enough to just prevent unloading under the highest loads possible from the shaker.

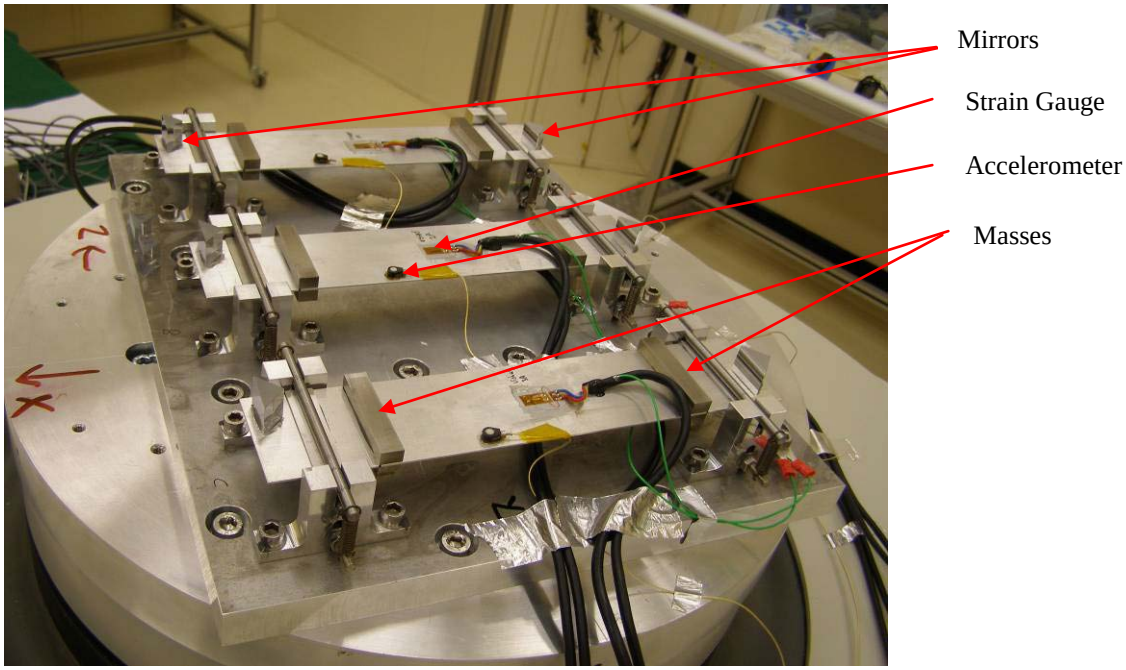

Figure 1 : Test setup.

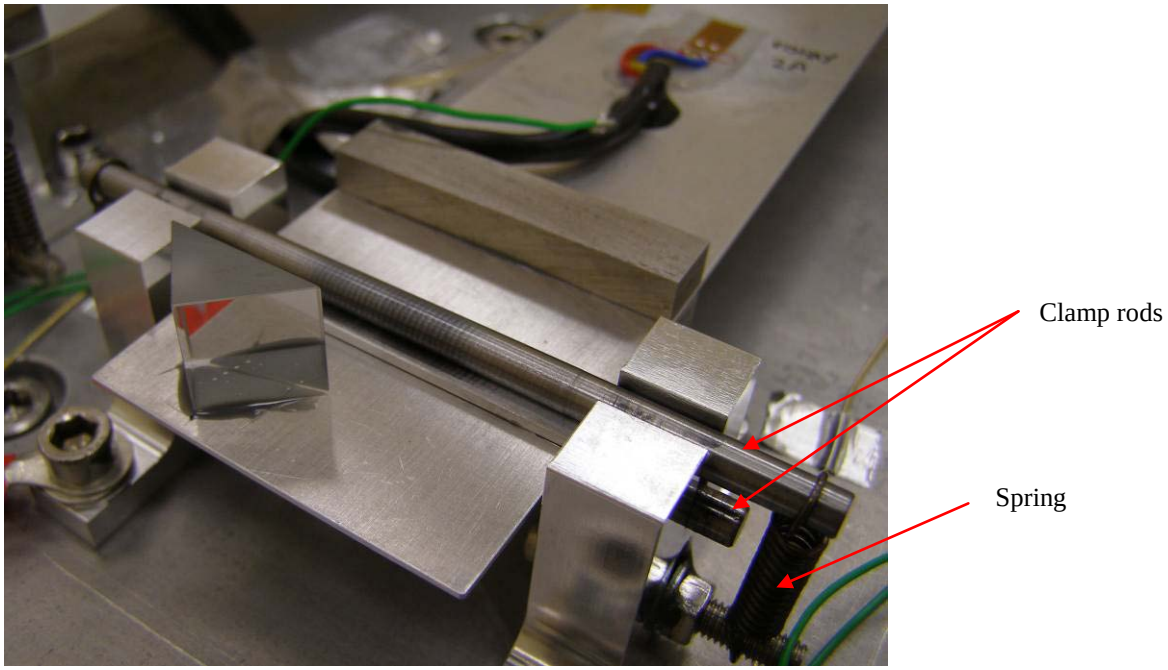

Figure 2 : Support clamp.

The random vibration loads were provided by the shaker. They started with very low level shakes, increasing in severity from 0.8 to 36 gRMS in increments of 3 or 6dB. The test spectra were based on the baseline shown in Table 1. This is similar to a typical verification test spectrum [1], though with the plateau starting at a fairly low frequency to ensure that it fully covers the first mode. Test durations were 60 s each.

Frequency	Level
20-30 Hz	+3dB/oct
30-200 Hz	0.1 g^2/Hz
200-2000Hz	-5dB/oct

Table 1 : Baseline test spectrum (6.44 gRMS).

Between each shake, metrology data were recorded to assess residual plastic strains in the samples as a result of the prior shake. This was accomplished with two separate methods – strain gauges and optical autocollimation. A pair of strain gauges was mounted on each test sample, one on the upper surface and one on the lower surface in the beam centre. Strain gauge resolution was quoted by the manufacturer to be ±0.25 μstrain. The optical method made use of a pair of mirrors at either end of the samples. The angle between these mirrors was measured very accurately with an autocollimator to derive an average bending strain along the samples. The resolution of this method was ±0.17 μstrain. Experimental errors due to the test setup were about +/-10 μstrain.

A fourth sample was subjected to static testing on a Testometric tensile test rig. The setup for this test was a four-point configuration, equivalent to the dynamic tests. The purpose of this test was to compare static and dynamic test data, and assess whether static test results in the microyield region could be used to predict dynamic results.

3 TEST RESULTS

The test results are summarized in Figure 3. There are several clear conclusions. Firstly, the low-level shakes (up to 13 gRMS) produce little discernable effect outside the error range. Secondly, at high levels, a definite trend in residual strains is observed – all samples start to show an increase in positive (tensile) residual strain for both top and bottom strain gauges. Effectively the samples are growing in length.

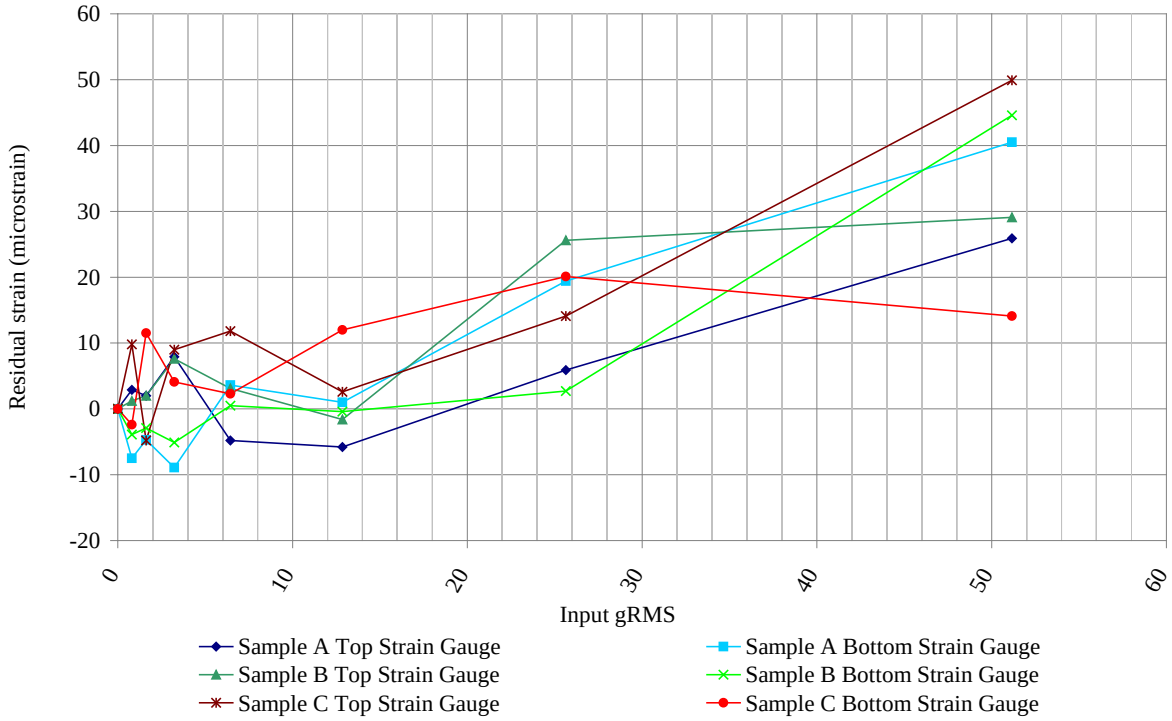

Figure 3 : Test results summary.

This result was somewhat unexpected – it was thought that the residual strains would be dominated by bending strains, which would be manifested in top and bottom strain gauges giving roughly equal and opposite responses. To better visualize the residual strain response, it was divided into a residual axial strain (from the average of the top and bottom strain gauges) and a residual bending strain (from the difference between them). These are shown in Figure 4 and Figure 5, in a traditional stress versus strain format. The RMS stress was obtained from the strain spectral density response of the strain gauges during the test.

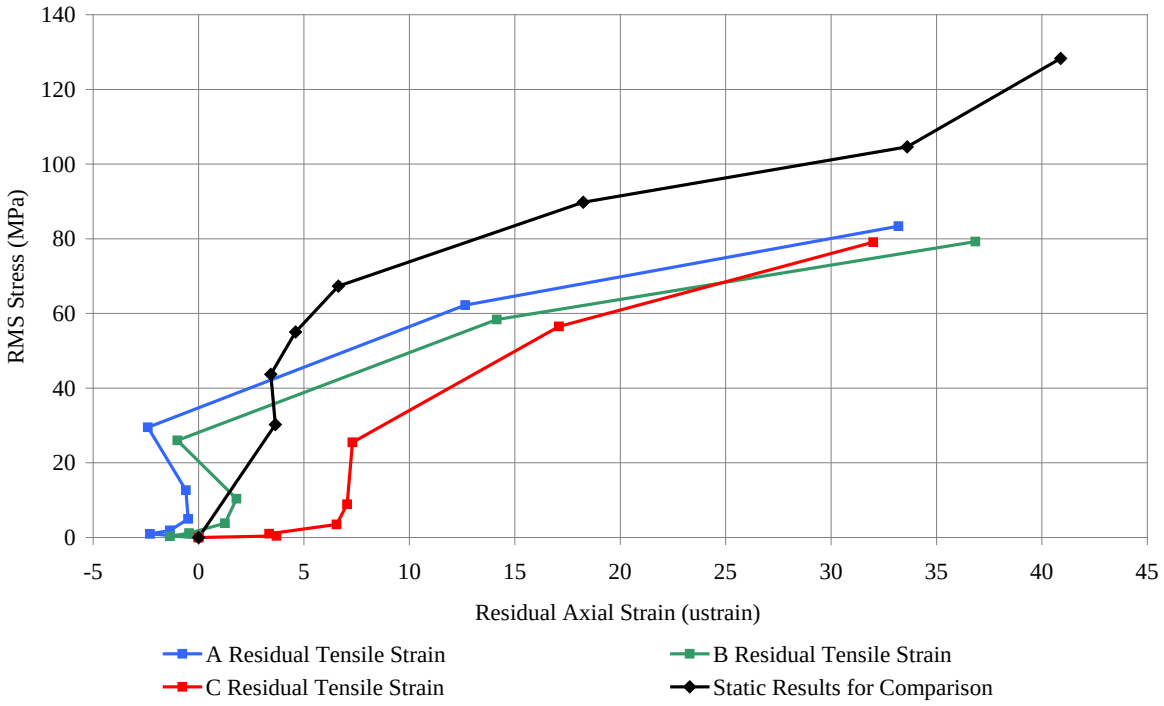

Figure 4 : Residual axial strain.

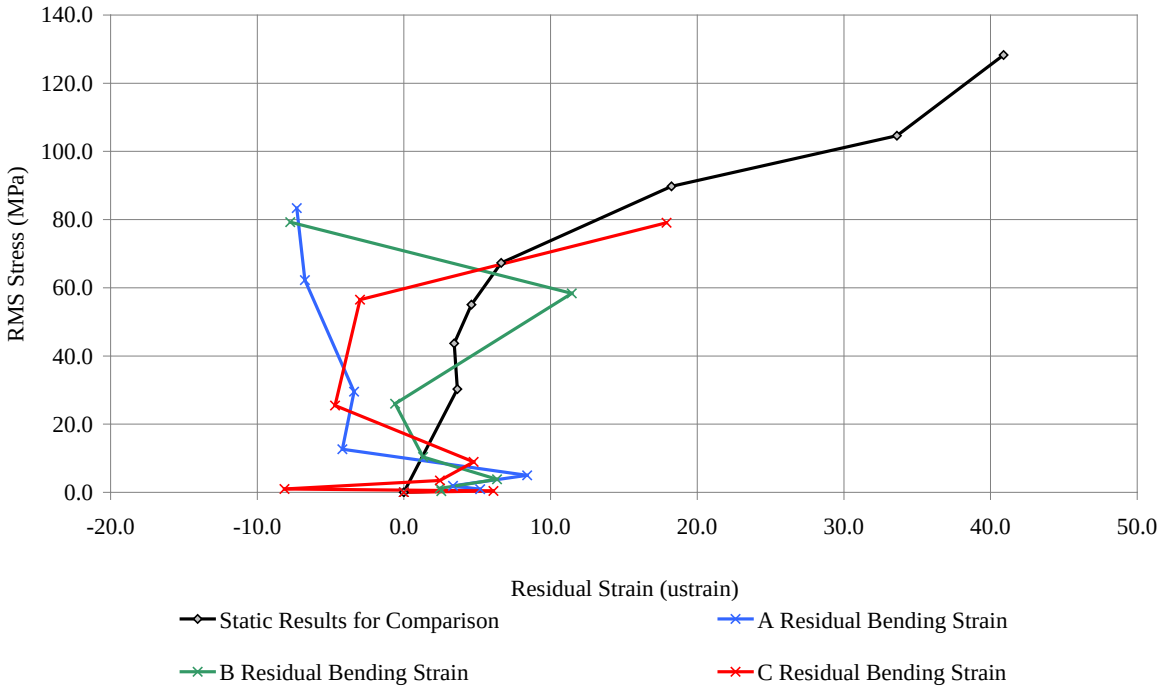

Figure 5 : Residual bending strain.

The axial strain results follow the same trend as the static test results, albeit at a lower stress level. The bending strain results generally increase in magnitude with increasing dynamic stress, but do not generally increase in the same direction.

As the test items are simply supported, the dynamic stresses are almost purely due to bending, with tensile stresses on one surface being equal and opposite to compressive stresses on the other. At the mounting positions, there is a small axial force due to friction between the test sample and the clamp rods. This force is very small by comparison though – for the penultimate dynamic test (25.6 gRMS), the RMS bending stress was 56 MPa, while the friction-induced axial component was only 0.5 MPa.

4 ANALYSIS

It was decided to investigate these results further using Finite Element Analysis, with cyclic plasticity material behaviour. It was assumed that the residual strain response was due to the first vibration mode, and that the contribution of higher modes to residual strain was negligible. ANSYS Version 12.1 was used, and the model was two-dimensional with large deformations and nonlinear material properties. The 25.6 gRMS test run was chosen for analysis, as this was the first run where a significant plastic strain response was seen. The results of Sample “B” were used.

There were two parts to the analysis. The first part was to correlate the model with the test results in order to validate the model and boundary condition assumptions. The second part was a time-domain analysis, with a large number of quasi-static load reversals applied to the model to simulate the time history of the stresses within the sample. The responses of the correlated model at the centre of the sample (where the accelerometer was located) and the FEA model are shown in Figure 6. The responses are well correlated for the first two modes, but

not after this (the difference in high frequency behaviour is probably due to the FEA model being only two-dimensional).

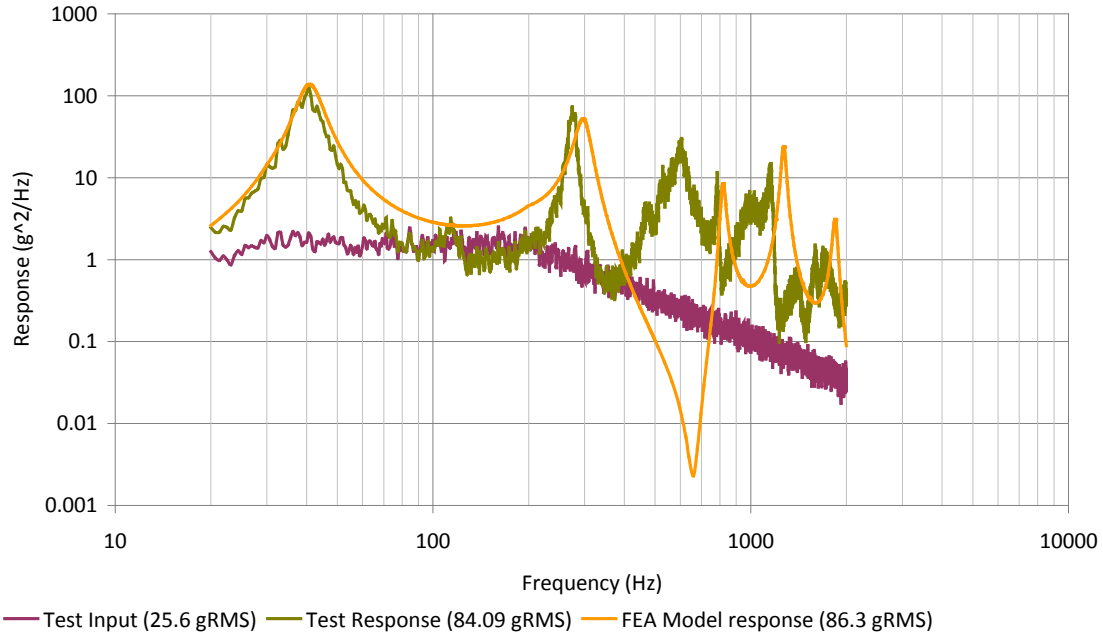

Figure 6 : Comparison between FEA model and test PSD responses.

The PSD response was then truncated between the first and second modes (at a factor of $\sqrt{2}$ from the first natural frequency). The RMS value of this truncated response was obtained, and assumed to be the quasi-static acceleration load applied to simulate the first modeshape for the static analysis (39.1 g). The FEA model with quasi-static loads applied is shown in Figure 7 and Figure 8. It contained 232 elements and 1658 degrees of freedom. It was constructed in two dimensions to minimize the solution time for a large number of sequential nonlinear solutions.

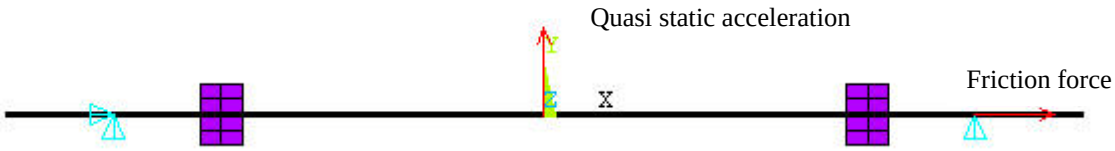

Figure 7 : FEA model showing quasi-static acceleration upwards

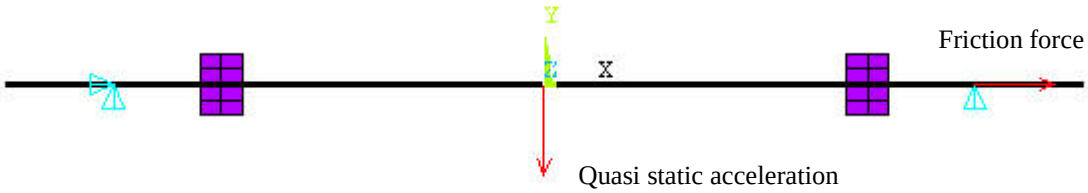

Figure 8 : FEA model showing quasi-static acceleration downwards

The X-direction stress response is shown in Figure 9, and enlarged in Figure 10. The stresses on the upper and lower surfaces (56.7 and 55.7 MPa) compare well with the RMS stress recorded by the strain gauges, of 58.9 and 57.9 MPa.

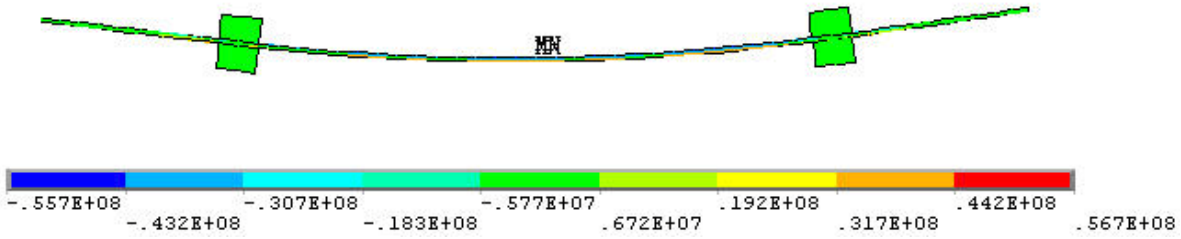

Figure 9 : Stress response to quasi-static acceleration

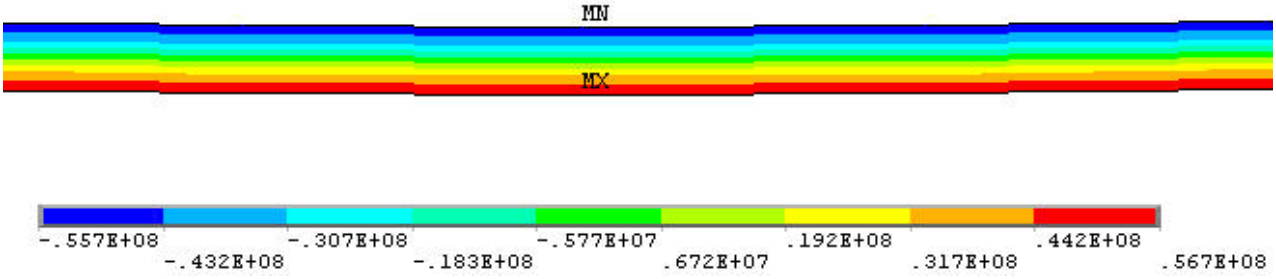

Figure 10 : Stress response enlarged at sample centre

To simulate the time history of the loads, an approach similar to Miner's rule [2] was taken. Load cycles of 1-σ, 2-σ and 3-σ (ie, 39.1, 78.2 and 117.3 g) were applied. The number of cycles of each were determined from the probability of exceedance multiplied by the total number of first mode cycles witnessed during the test (the natural frequency multiplied by the test duration). The number of fully reversed cycles was 779, 112 and 7 for the 1-σ, 2-σ and 3-σ cases respectively.

To model material cyclic plasticity, it was decided to use the nonlinear kinematic hardening model of material behaviour [3]. This model was chosen for several reasons – it was a supported material model in the FEA code used; it can effectively model plastic strain evolu-

tion effects such as ratchetting and shakedown; some material data can be found in the literature for materials similar to the one tested here.

The model requires three basic parameters to be defined: k, C_i and γ_i. Here, k is the elastic limit or yield stress, C_i is the initial hardening modulus, and γ_i is a parameter that controls the rate at which the hardening modulus decreases with increasing strain. All three parameters are best determined from cyclic stress tests where a stable hysteresis cycle is obtained for several levels of plastic strain of interest. Additional values of C_i and γ_i (representing additional kinematic models) can be superimposed to better represent additional strain ranges. In this case, two superimposed kinematic models were used - C_1 and γ_1 were obtained from the static test data using a "goal-seek" spreadsheet function (representing a very low range of plastic strain, 10^{-6} – 10^{-5}) and C_2 and γ_2 were obtained from [4] for alloy 2024 T4 (for a much higher strain range, above about 10^{-3}). It should be noted that the static test data used to determine C_1 and γ_1 was monotonic – ideally this would have been cyclic. The superimposed model is shown in Figure 11, along with test data and the model from [4]. As the first kinematic model is based on test data only up to about 40 μstrain (plastic), and the second is intended for a much higher strain range, there is effectively a gap in the validity of this model after about 40 μstrain. Fortunately, most of the dynamic stress effects observed in this test are covered in the lower strain range. The material constants used are summarized in Table 2.

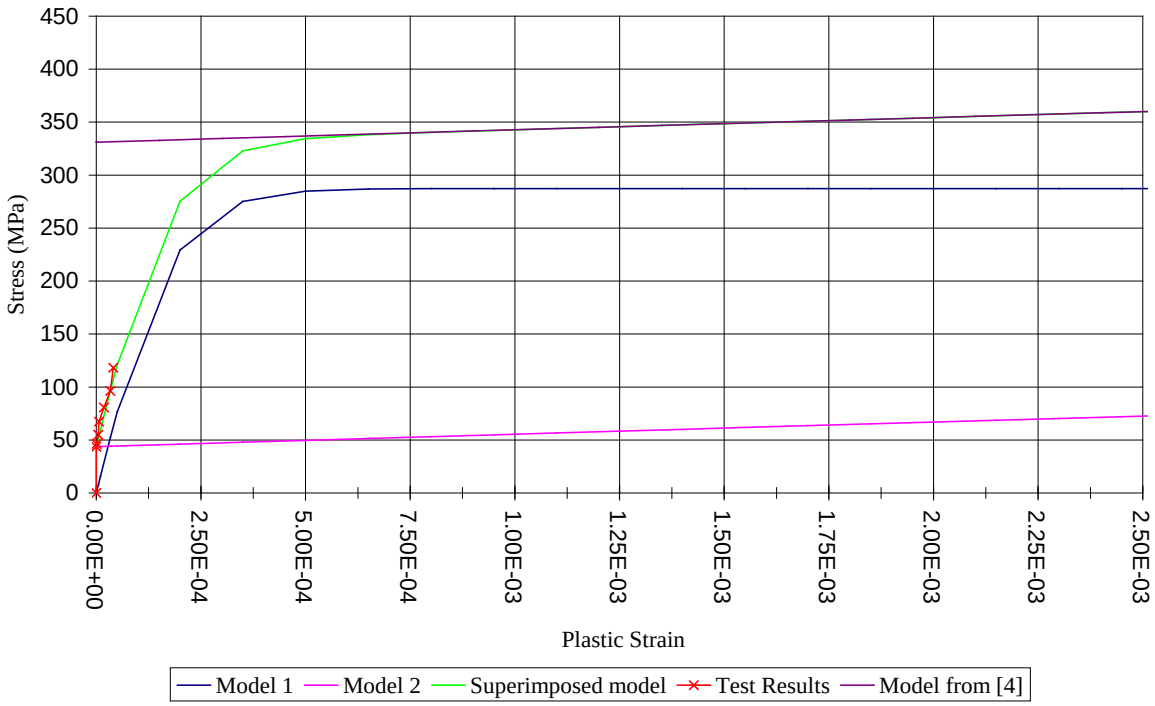

Figure 11 : Determination of material constants

Constant	Value	Units
k	4.37e7	Pa
C_1	6.57e12	Pa
γ_1	2.29e4	-
C_2	1.18e10	Pa
γ_2	1.03e2	-

Table 2 : Material constants

For ease of load application, the cycles were applied in groups of the same level – ie, the 3-σ cycles were applied first, followed by the 2-σ and 1-σ cycles. The results are shown in Figure 12 for a node in the same location as the strain gauge on the upper surface.

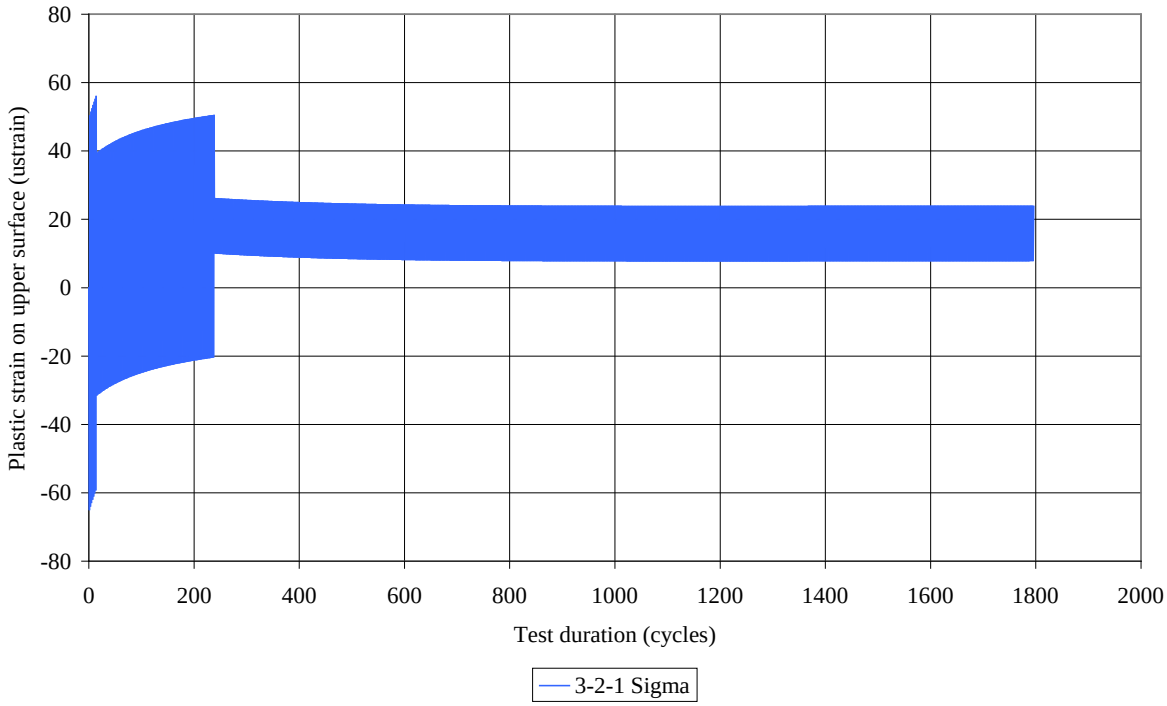

Figure 12 : Plastic strain results

There are several points to note about this curve. Firstly, the plastic strain amplitudes are high (as expected) for the 3-σ case, in the region of ±57 μstrain. This reduces to about ±8 μstrain for the 1-σ case. Secondly, shakedown is apparent. This is mostly complete following the 2-σ case, and results in a mean plastic strain of around 16 μstrain. As this mean plastic strain is positive, the trend is for a growth in length of the sample, as witnessed during testing. The mean value from testing, effectively the average of residual strain on the upper and lower surfaces, is 14 μstrain (from Figure 4). Thus there is also a good agreement with the level of residual axial strain.

The difference between upper and lower surface residual strain was 23 μstrain under testing. From results in Figure 12, it is clear that the equivalent FEA results are somewhat dependent on the level of the final stress cycle, in this case 1-σ. Here, the difference is 16 μstrain, suggesting that a level slightly higher than 1-σ would have been appropriate for this last cycle.

5 MORE COMPLEX STRUCTURES

It is proposed that the method applied here could be used for more complex structures, such as a mirror mounted on flexures that requires very high levels of dimensional stability following random vibration exposure. For such structures, a fully kinematic mounting design may mean that structural pre-stresses are low. However the results of this test have shown that even a low level of stress asymmetry in cases where peak stresses exceed the material's elastic limit can lead to significant residual strain. Also, gravity and static launch accelerations may be important.

For a complex structure, the first modeshape must firstly be determined with some accuracy. Next, acceleration loads must be determined that generate a deformed shape that approximates this modeshape. This will necessarily be an approximation – even for the simple geometry described in this paper, the first modeshape is not identical to the deformed shape under static acceleration. Next, the magnitude of the acceleration loads should be adjusted so that the deflections are equivalent to 1-σ deflections from a random vibration run. These accelerations can finally be applied in reversed cycles at several levels (ie 1-σ, 2-σ etc) with the commensurate number of cycles. For areas where microyield is expected, the material properties must include nonlinear kinematic hardening. This will probably mean a bespoke material test, as there appears to be a paucity of data in the literature for these levels of plastic strain. A single kinematic model would probably suffice unless a very large range of stresses above the elastic limit is expected. A final issue to tackle will be determining the number of cycles to apply for each load level. Nonlinear kinematic hardening makes use of the von Mises ductile failure criterion. It is a well known problem in random vibration analysis that von Mises equivalent stresses are do not observe a Gaussian probability density function, even if the component x, y and z stresses do. However there are methods to determine or estimate the correct von Mises probability density function [5], [6] that could be applicable.

6 CONCLUSION

Aluminium strip samples in a four-point bending configuration were subject to random vibration in order to assess their dimensional stability. At moderate levels of dynamic stress, the samples exhibited significant residual strain along the length of the strip. A finite element model using nonlinear kinematic hardening material properties was produced to investigate this behaviour. This model was solved in the time domain with a number of reversed load cycles superimposed on a small frictional force. The results of this analysis exhibited a shakedown effect which agreed well with the test observations. This method of analysis has been proposed for more complex structures with high dimensional stability requirements.

REFERENCES

[1] "Space Engineering—Testing," ESA, European Space Research and Technology Centre, Rept. ECSS-E-10-03A, Noordwijk, The Netherlands, 2002.

[2] J.E. Shigley, "Mechanical Engineering Design", McGraw-Hill, 1986.

[3] J. Lemaitre, J-L. Chaboche, "Mechanics of Solid Materials", Cambridge University Press, 1990.

[4] M.L.M. Francois, "A Pasticity Model with Yield Surface Distortion for Non Proportional Loading", International Journal of Plasticity, Vol. 17, No. 5, pp. 703 - 718, 2001.

[5] D. Segalman, G. Reese, R. Field Jr., C. Fulcher, "Estimating the Probability Distribution of von Mises Stress for Structures Undergoing Random Excitation", Transactions of the ASME, Vol. 122, 2000.

[6] De la Fuente, "Von Mises Stresses in Random Vibration of Linear Structures", Computers and Structures, Vol. 87, Iss. 21-22, 2009.